

Article

Visualized Experimental Study of Soil Temperature Distribution around Submarine Buried Offshore Pipeline Based on Transparent Soil

Hui Li ^{1,2} , Yajing Meng ^{1,3}, Yilong Sun ^{1,4,*}  and Lin Guo ^{1,2}

¹ College of Civil Engineering and Architecture, Wenzhou University, Wenzhou 325035, China; lihui21@163.com (H.L.); mengyajing99@foxmail.com (Y.M.); lingpray@126.com (L.G.)

² Key Laboratory of Engineering and Technology for Soft Soil Foundation and Tideland Reclamation of Zhejiang Province, Wenzhou 325035, China

³ Zhejiang Engineering Research Center of Disaster Prevention and Mitigation for Coastal Soft Soil Foundation, Wenzhou 325035, China

⁴ Collaborative Innovation Center of Tideland Reclamation and Ecological Protection, Wenzhou 325035, China

* Correspondence: sunyilong@wzu.edu.cn

Abstract: The temperature distribution around the offshore burial pipeline is an important factor affecting its safety design and economic operation. The traditional test method cannot obtain the continuous temperature distribution of soil owing to the constraints of placing measurement sensors in soil. The transparent soil model test is an alternative method to realize the visualization research of soil temperature. In this paper, a relationship between the temperature of transparent soil and pixel intensity was first established. Then, the transparent soil test and numerical simulation, considering the natural convection, were carried out to study the temperature distribution around the submarine pipeline during start-up and stable operation. The influence of buried depth and pipeline diameter was analyzed. The results suggest that the continuous temperature distribution can be obtained visually by using a transparent soil test, and the observed heating zone of influence extended to a radial distance of 2.6 pipe diameters. The numerical analysis results show that the influence zone of the temperature of pipeline is a distance of four pipeline diameters at a temperature difference of 45 °C. The buried depth and pipeline diameter have little influence on the influence zone. In addition, the contour curves of soil temperature around the pipeline with different diameter are similar in shape. With the decrease in the buried depth of pipeline, the temperature gradient of soil around the pipeline decreases, which is caused by the natural convection.

Keywords: offshore pipeline; transparent soil; thermal field; numerical simulation



Citation: Li, H.; Meng, Y.; Sun, Y.; Guo, L. Visualized Experimental Study of Soil Temperature Distribution around Submarine Buried Offshore Pipeline Based on Transparent Soil. *J. Mar. Sci. Eng.* **2024**, *12*, 637. <https://doi.org/10.3390/jmse12040637>

Academic Editor: Atilla Incecik

Received: 18 March 2024

Revised: 7 April 2024

Accepted: 8 April 2024

Published: 9 April 2024



Copyright: © 2024 by the authors. Licensee MDPI, Basel, Switzerland. This article is an open access article distributed under the terms and conditions of the Creative Commons Attribution (CC BY) license (<https://creativecommons.org/licenses/by/4.0/>).

1. Introduction

Offshore buried pipelines are often used in transportation engineering of marine crude oil with the advantages of low cost, large transportation volume and continuous transportation. Crude oil produced from offshore fields usually has a high wax content, resulting in poor fluidity at the marine environmental temperature. To ensure the smooth and safe transportation of crude oil, it is often raised to a very high temperature. However, the sea water temperature decreases with the increase in water depth. The temperature of sea water at 2000 m depth is about 3 °C [1]. There is a large temperature difference between the pipeline and the surrounding environment, which means that the heat of the pipeline transmits to the surrounding soil. Heat transmission causes the temperature of oil to drop, which, in turn, affects its transportation. In addition, it changes the temperature of the soil around the pipeline, which effects the interaction between the pipeline and soil. There is a huge impact on the safety and stability of the pipeline. It is very important to have a thorough understanding of the soil temperature distribution around the pipeline, which is

an important basis for the safe design and economic operation of the pipeline. Therefore, it is necessary to study the soil temperature distribution around the pipeline.

Subsea burial is a common method to prevent pipeline damage and heat loss for submarine pipelines. The heat transfer of the buried pipeline is an important and complex problem. In the previous research on the temperature distribution of soil around the buried pipeline, the influence of the thermal conductivity of the insulation layer, properties and geometric properties of backfill materials, soil stratification, soil moisture content and void ratio, natural convection and other factors were studied by using numerical and experimental methods [2–6]. However, the experimental test usually uses temperature sensor embedded in the soil to measure the soil temperature. The temperature measurement has spatial discontinuity. The measurement is not accurate under large temperature gradient, such as media stratification, natural convection and local material phase change. In most numerical simulations, the soil is assumed to be solid material, ignoring the porous media characteristics of soil.

Transparent soil test technology can realize the visualization of the displacement of soil. The previous studies of transparent soil test mainly focus on the physical and mechanical properties of transparent soil materials [7–11] or use transparent soil tests to study the deformation of soil around the pile, tunnel, anchor or other structures [12–16]. The transparency of the transparent soil is expected to be improved for larger model tests. The changes in transparency caused by temperature, saturation and impurities are considered to be unfavorable factors in the transparent soil test; these factors need to be strictly controlled in the test. However, the change in the transparency of transparent soil can also be a favorable factor in the test [17,18]. Based on this understanding, the relationship between transparency of transparent soil and temperature was established through experiments, and the temperature field around the energy pile was studied [17]. It was proved that the continuous temperature field around the structure could be obtained based on the change in the transparency of transparent soil.

Therefore, aiming at studying the discontinuity of temperature monitoring in the traditional experimental test for the thermal fields of the submarine buried pipeline, a visual model test of the soil temperature distribution around the submarine buried pipeline by using transparent soil model test was carried out. The temperature distribution of soil around the submarine buried pipeline during operation was analyzed. Combined with the numerical simulation, the effect of the buried depth and pipe diameter on the soil temperature distribution around the submarine pipeline was studied.

2. Test Method and Process

2.1. Test Method for Transparent Soil

Transparent soil consists of transparent solid particles and a fluid with a matching refractive index. The matching degree of the refractive index between solid particles and pore fluid is one of the main factors affecting the transparency of transparent soil. The refractive index of a material is usually affected by the wavelength of light and temperature. The refractive index of solid particles is generally considered not to vary with temperature. However, the refractive index of fluid varies greatly with temperature. Kong et al. [19] measured the variation in the refractive index of fluid that may be used in the transparent soil model test with temperature. It found that the refractive index of those pore fluids mostly decreased with the increase in temperature. Therefore, with the variation in temperature, the matching degree of refractive index between solid particles and pore fluid decreases, resulting in the decrease in the transparency of transparent soil. The previously transparent medium becomes opaque or appear less clear with the change in temperature.

Individual pixels are the smallest unit that forms a digital image. The pixel intensity is used to describe the color and brightness of the pixels. The most commonly used pixel format is where the pixel number is stored as an 8-bit integer. The corresponding decimal values range from 0 (black) to 255 (white). When the pixel intensity is between the two extreme values, the pixel will appear gray, as shown in Figure 1. We prepared

the transparent soil at the specified temperature (i.e., 20 °C) with the optimum refractive index match. We placed a black background behind the transparent soil and shot it through the soil. At this time, the black background was clearly visible as the soil was transparent. The pixel intensities of the background were sufficiently low due to the relative high transparency of the transparent soil. Conversely, when the temperature of the transparent soil increased (i.e., 50 °C), the transparency of transparent soil decreased due to the reduction in refractive index matching degree. The pixel intensity increased such that the soil appeared to be gray in color. Therefore, the visual measurement of transparent soil temperature could be achieved by establishing the relationship between pixel intensity and the temperature of transparent soil.

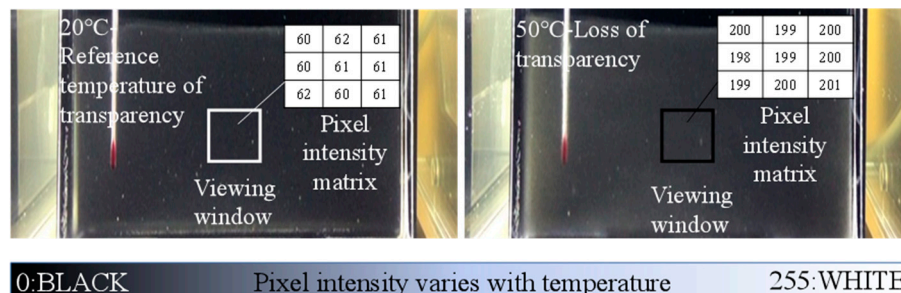


Figure 1. The measurement of temperature in transparent soil.

2.2. Test Materials

The transparent soil material used in this study was manufactured using fused quartz and mixed oil. Fused quartz is a commonly used solid particle material for transparent soil configuration due to its high purity, high transparency, high angular and similar chemical composition to natural sand [20]. The particle size distribution of the fused quartz is shown in Figure 2, which is close to that of natural marine sand [21–23]. The mixed oil was a blend of mineral oil (white oil) and paraffinic solvent (Norpar 12) with a mass ratio of 4:1. The refractive index of mixed oil is 1.4585 at 20 °C, which is consistent with that of fused silica. The fused quartz and mixed oil were thoroughly mixed by using a blender to form a uniform slurry. The sample was then placed in a vacuum to evacuate the air. A two-phase continuum was produced, which enabled the transparency of the transparent soil. The other specific preparation process of transparent soil is presented in the literature [24]. The physical and mechanical parameters of the transparent soil are shown in Table 1.

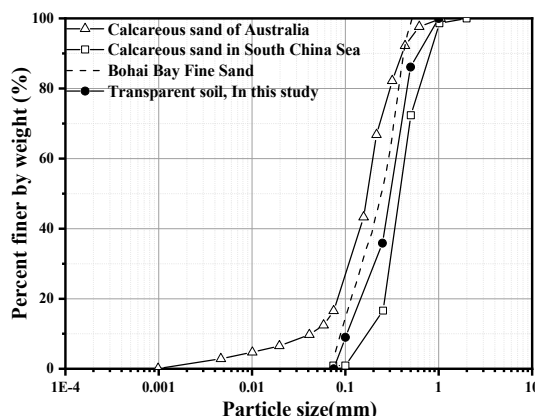


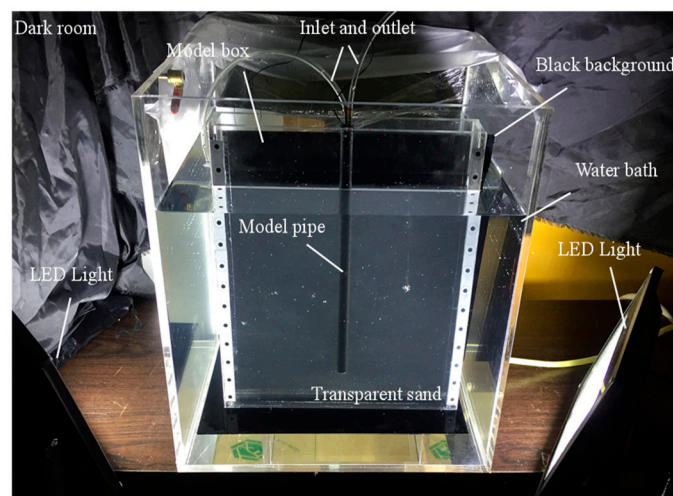
Figure 2. The particle distribution of fused quartz and natural marine sand including calcareous sand of Australia [21], calcareous sand in South China Sea [22], and Bohai Bay fine sand [23].

Table 1. Mechanical properties of the transparent soil.

Parameter	Unit	Value
Nonuniformity coefficient, C_u		3.51
Curvature coefficient, C_c		1.14
Saturated bulk density, $\gamma_{t,sat}$	kg/m ³	18.37
Thermal conductivity, K_t	W/(m·K)	0.785
Specific heat capacity, C_t	J/(kg·K)	2097.90

2.3. Test Apparatus for Transparent Soil

The visualization test apparatus for the submarine pipeline temperature based on transparent soil is shown in Figure 3. The test system mainly includes water bath, LED lighting device, temperature control device, model pipe, model box, image acquisition device and other parts. The water bath with dimensions of 400 mm (length) by 400 mm (width) by 450 mm (height) was mainly used to provide a constant temperature boundary for the model box filled with transparent soil. The water bath was filled with water, which was warmed by the temperature control device. The temperature control device includes a heating/cooling element and a circulating water pump to achieve a constant temperature of the water bath through the circulation of water. The model box for the transparent soil is 300 mm × 40 mm × 350 mm in size and constructed of 10 mm thick plexiglass panels. The model pipe was manufactured by using hollow copper pipe with black surface spraying. A water inlet and outlet were arranged in the inner space of the pipe. The inlet and outlet were connected with another temperature control device. The temperature of the pipe was controlled through the circulation of water inside the pipe. The specific dimensions and relative positions of the model box and model pipe are shown in Figure 4.

**Figure 3.** The physical figure of visual test system of offshore pipeline temperature.

Nonuniform lighting conditions are not conducive to producing consistent pixel intensity. In order to produce a consistent background, the test device was placed in a dark room. Two LED lights with constant power were used to provide uniform illumination of the water bath and model box. A CCD high-speed high-definition camera with fixed aperture, exposure time and focus was used to record the test image. During the test, the CCD camera was installed on a tripod at a distance of 0.5 m from the front of the water bath. The CCD camera was connected to the computer. The images of the test were captured without contact through control the software on the computer, which ensures long-term testing without operator intervention. The temperature field around the model pipe can be obtained through the image analysis software.

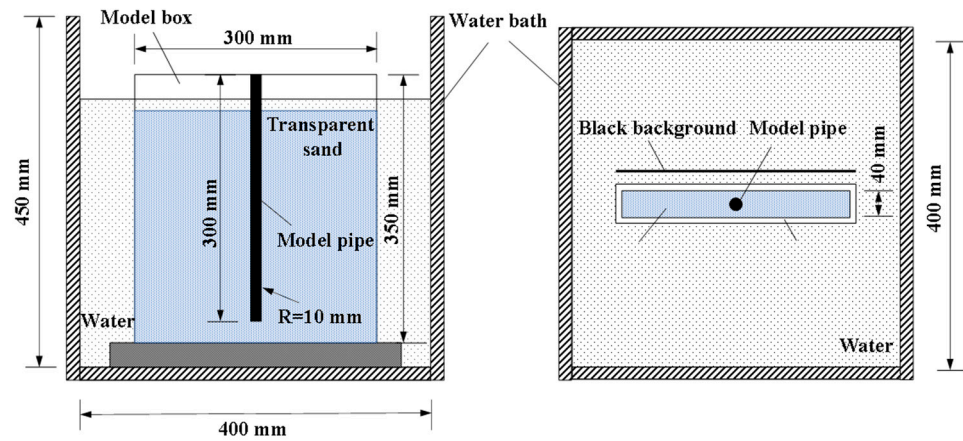


Figure 4. The schematic diagram of model tank in a transparent soil temperature test.

2.4. Numerical Simulation Method

(1) Mathematical model

As pipes are always longer than they are wide, a two-dimensional plane model of the buried submarine pipeline was used in this study, as shown in Figure 5. The length and depth of the rectangular influence range of the pipeline on the soil temperature distribution is $2a$ and b , respectively. The pipe section is circular with diameter of D and buried depth of H . The coordinate system is established with the corresponding center point of the pipeline on the seabed surface as the origin. The horizontal direction is the x -axis, and the vertical direction is the y -axis. The sea water temperature above the seabed surface is T_w . The initial temperature of soil is $T_{s,ini}$. The thermal conductivity of soil is K_s . There is thermal convection between the seabed surface and seawater, including natural convection.

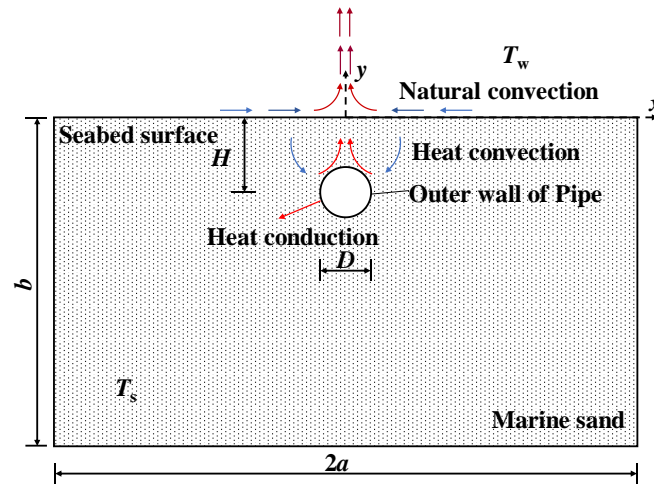


Figure 5. The two-dimensional plane model of heat transfers of offshore pipeline.

In order to simulate the physical process of heat transfer from the pipeline to the surrounding soil during start-up and operation, the following governing equations were used in the numerical model. Fourier’s law expresses the conductive heat flux as a function of the temperature gradient as follows:

$$\mathbf{q} = -K\nabla T \tag{1}$$

The heat transfer in the soil, which is considered to be a porous medium, is governed by the heat transfer equation:

$$\rho C \frac{\partial T}{\partial t} + \nabla \cdot (-K \nabla T) = Q \tag{2}$$

The initial condition is that the temperature of soil is $T_{s,ini}$ for $t = 0$.

The thermal boundary conditions are that the temperature of the outer wall of the pipeline is constant as T_{wall} . The left, right and lower boundaries are adiabatic boundaries. The upper boundary is the heat flux boundary, and there is natural convection between the seabed surface and seawater. The convective heat flux is

$$q_0 = h(T_w - T) \tag{3}$$

The convective heat transfer coefficient h is determined by the following equation:

$$h = \begin{cases} \frac{K}{2a} 0.54 R_a^{1/4} & \text{if } T > T_w \text{ and } 10^4 \leq R_a \leq 10^7 \\ \frac{K}{2a} 0.15 R_a^{1/3} & \text{if } T > T_w \text{ and } 10^7 \leq R_a \leq 10^{11} \\ \frac{K}{2a} 0.27 R_a^{1/4} & \text{if } T \leq T_w \text{ and } 10^4 \leq R_a \leq 10^7 \end{cases} \tag{4}$$

It should be noticed that there is a sudden rise in the temperature of the outer wall of the pipeline at the beginning of the numerical simulation. In Table 2, all the employed parameters for the equations are reported.

Table 2. The employed parameters for the equations.

Symbol	Parameter	Unit
C	Specific heat capacity of material	J/(kg·K)
D, H	Diameter and buried depth of pipeline	m
h	Convective heat transfer coefficient	W/(m ² ·K)
K	Thermal conductivity of material	W/(m·K)
ρ	Density of material	
Q	Heat	J
q_0	Heat flux	W/m ²
q	Heat flux vector	W/m ²
T	Temperature of material	K
R_a	Reynolds number	

(2) Numerical solution

The software of COMSOL Multiphysics 5.2 was employed to study the soil temperature distribution around the pipeline during stable operation, considering the natural convection.

To ensure the calculation of the model, the model was subject to the following assumptions: (1) the influence area of the pipeline on the surrounding soil was a rectangular area; (2) the soil was a continuous and uniform porous medium, and the soil was saturated and the pore water does not change phase; (3) the thermodynamic parameters of soil were kept constant and did not change with temperature; (4) the flow in soil was two-dimensional and followed Darcy’s law; (5) there was no heat exchange between the soil skeleton and pore water; (6) the thermal conductivity of soil was independent of temperature; (7) the water in soil did not evaporate; (8) there was a natural convection between the seabed and seawater.

A two-dimensional pipe-soil model was used in this study, which means that the change in the pipeline temperature in the axial direction was not considered. Considering the boundary effect, the length of the model was set to 16 m, and the depth was set to 8 m. The section of pipeline was circular. The diameter D and buried depth H of the pipeline were set according to different test conditions. The soil material used in the numerical simulation was fine sand from the South China Sea, which was described as a porous medium saturated by water. The physical properties of the soil and seawater are

shown in Table 3. To consider the natural convection between the soil and the seawater, the upper boundary was defined as the heat flux boundary. The left, right and lower boundaries were defined as adiabatic boundaries by setting the heat flux conditions as zero. At the beginning of the simulation, the soil temperature was assumed to be uniform and constant $T_{s,ini}$, which was same as the temperature of the seawater T_w . After heating, the soil temperature changed. In fact, we were interested in studying heat transfer from the outer surface of the pipe to the soil, rather than solving for the fluid flow inside the pipe. Therefore, the temperature of the outer wall of the pipe was set to the constant and uniform temperature T_{wall} . Due to the existence of temperature difference between the pipeline wall and soil, the heat of the pipeline continued to transfer to the soil, which meant that the soil was heated.

Table 3. Mechanical properties of the soil.

Soil Mass	Parameter	Unit	Value
Marine sand	Thermal conductivity, K_s	W/(m·K)	0.867
	Specific heat capacity, C_s	J/(kg·K)	3465
	Bulk density, γ_s	kg/m ³	18.0
	Porosity, n		0.6
Seawater	Thermal conductivity, K_w	W/(m·K)	0.65
	Specific heat capacity, C_w	J/(kg·K)	3850
	Bulk density, γ_w	kg/m ³	10.25

The specific mesh division used in the model is shown in Figure 6, where the mesh is finer near the pipe to ensure the convergence of numerical calculation and accuracy of the simulation. The triangular elements are used in the model, which are linear. The discretization of the domain has a total of 537 nodes and 979 elements.

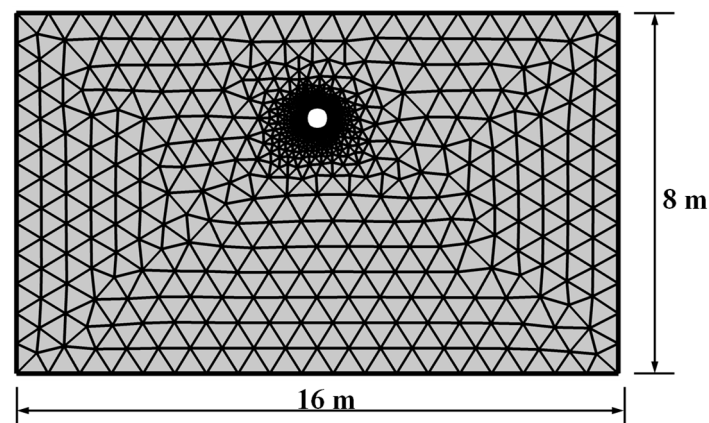


Figure 6. FEM mesh of numerical model.

2.5. Test Procedures and Progresses

In order to establish the relationship between the temperature of the transparent soil and the pixel intensity, the calibration test was carried out. Calibration of pixel intensity at different soil temperatures was achieved by placing the model box in the water bath and allowing the water circulation system to heat up. During the calibration test, the temperature of the water bath continuously increased from 20 °C to 50 °C, which was divided into 6 stages in 5 °C increments. At each heating stage, the temperature of the water bath was set to the desired value. The temperature of the soil was then precisely determined using a thermometer placed inside the model box. Images were captured during the heating process with an image acquisition frequency of 30 s. The image pixel intensities were obtained and recorded by using image processing software. Then, the relationship between pixel intensity and temperature were established.

To study the expansion of soil temperature around the pipeline along the horizontal direction, a transparent soil test was carried out to visualize the temperature. During the test, the temperatures of the outer wall of the model box filled with transparent soil and the model pipe were maintained at 20 °C and 50 °C, respectively, through the circulation of water warmed by the individual temperature control device. Due to the thin outer wall of the model pipe and the high thermal conductivity of copper, the pipe increased to the required temperature in a short time, which was not taken into account during the test. During the test, the images of the transparent soil were captured at a frequency of 5 min depending on the nature of the test. The measures ensured that sufficient changes in pixel intensity of each pixel were monitored. The variation in pixel intensity in the image was interpreted as changes in soil temperature according to the established relationship between pixel intensity and soil temperature. Therefore, the visualization of the temperature could be achieved.

Numerical simulation was carried out to study the soil temperature distribution around the pipeline under different buried depths and pipe diameters, considering natural convection. In order to verify the validity of the model, the soil parameters and initial conditions for the transparent soil test were first used by the model, including the thermal conductivity and initial temperature of the soil (20 °C) and the temperature of the model pile (50 °C). The results of the numerical simulation were compared with those of the transparent soil test. After the verification stage, the parameters of marine sand were substituted into the model for the numerical simulation. The specific calculation conditions of numerical simulation are shown in Table 4. Combined with reference [25], the calculation time of the model was 60 days. For heat transfer analysis during start-up, 4 temperature monitoring points (named as point 1, 2, 3, 4, respectively) were set in the center of the pipeline along the horizontal direction of the model, with the distances far away from the outer wall of the pipe being 0.5, 1, 1.5, and 2 pipe diameters, respectively, as shown in Figure 7.

Table 4. Modeling case in numerical simulation.

Temperature (°C)	Buried Depth (H/D)	Pipe Diameter (m)
$T_w = 5$	0	0.6
$T_{s,ini} = 5$	1.0	0.8
$T_{wall} = 50$	2.0	1.0
	3.0	1.2

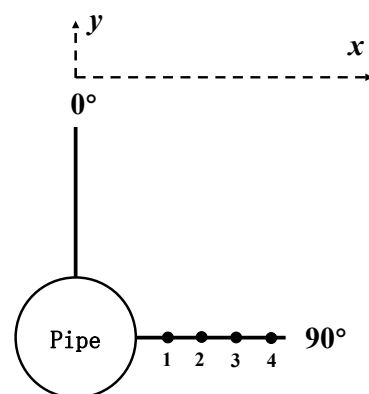


Figure 7. Distribution of temperature monitoring points for soil around the pipeline.

3. Experimental Results and Discussion

3.1. Calibration Test

The observation of transparent soil temperature is very sensitive to the change in image pixel intensity. In order to reduce the influence of abnormal pixel intensity on the test

results, it is necessary to normalize the pixel intensity. The normalization method proposed by Siemens et al. [18] is chosen in this study:

$$I_N = \frac{I - I_{\text{cold}}}{I_{\text{hot}} - I_{\text{cold}}} \tag{5}$$

where I_N is the normalized pixel intensity, I is the pixel intensity at the specified temperature, I_{cold} is the reference pixel intensity at low temperature and I_{hot} is the reference pixel intensity at high temperature.

The relationship between temperature and normalized pixel intensity is shown in Figure 8. It can be seen that the normalized pixel intensity varies from 0 to 1 for the temperature of 20 °C to 50 °C. The temperature of transparent soil has a logarithmic relationship with the normalized pixel intensity. The specific equation is as follows:

$$T = 48.839I_N^{0.163} \tag{6}$$

when the temperature is lower than 30 °C, the deviation between temperature data is apparent. It may be because the refractive of pore fluid is not sensitive to the variation in temperature at a lower temperature, resulting in low transparency changes. However, it is interesting to note that these results are in good agreement with the previous results [17,26]. The results of Siemens et al. [18] and Black et al. [17] are also listed in the figure. Siemens et al. [18] found a linear relationship between temperature and normalized pixel intensity in the test. Black et al. [17] found that the relationship curve between temperature and normalized pixel intensity is about a straight line when the temperature is greater than 30 °C, but it is nonlinear when the temperature is 20~30 °C. The variation in pixel intensity mainly depends on the change in the refractive index of pore fluid. Moreover, the research proposed by Kong et al. [19] showed that the refractive index of fluid was not uniformly sensitive to temperature. The difference of these test results may be caused by the difference in the pore fluid of transparent soil. Therefore, for the transparent soil prepared using different materials and processes, the relationship between temperature and normalized pixel intensity should be re-determined.

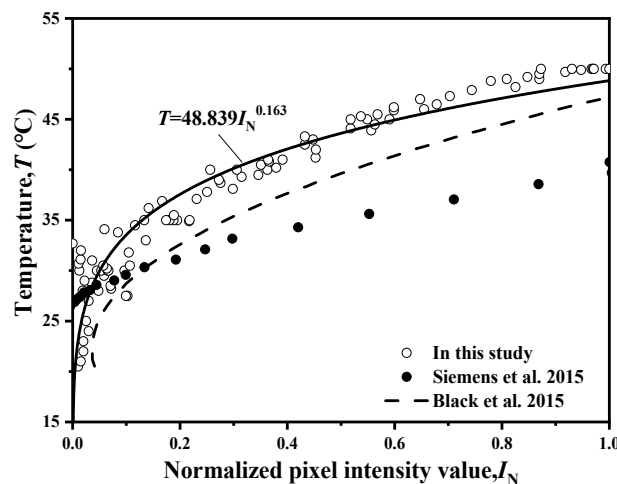


Figure 8. The relationship between temperature and normalized pixel intensity and the comparison with previous researches [17,18].

3.2. Horizontal Temperature Distribution of Soil around Pipeline

The test results of the horizontal temperature distribution of the submarine pipeline are shown in Figure 9. It can be seen from the figure that the temperature decreases with the increase in the distance from the pipe wall. After 5 min, the temperature expands to 0.5D. The influence range of pipeline temperature increases gradually with the increase in time. The influence range extends to 2.6D after 40 min, and tends to be stable.

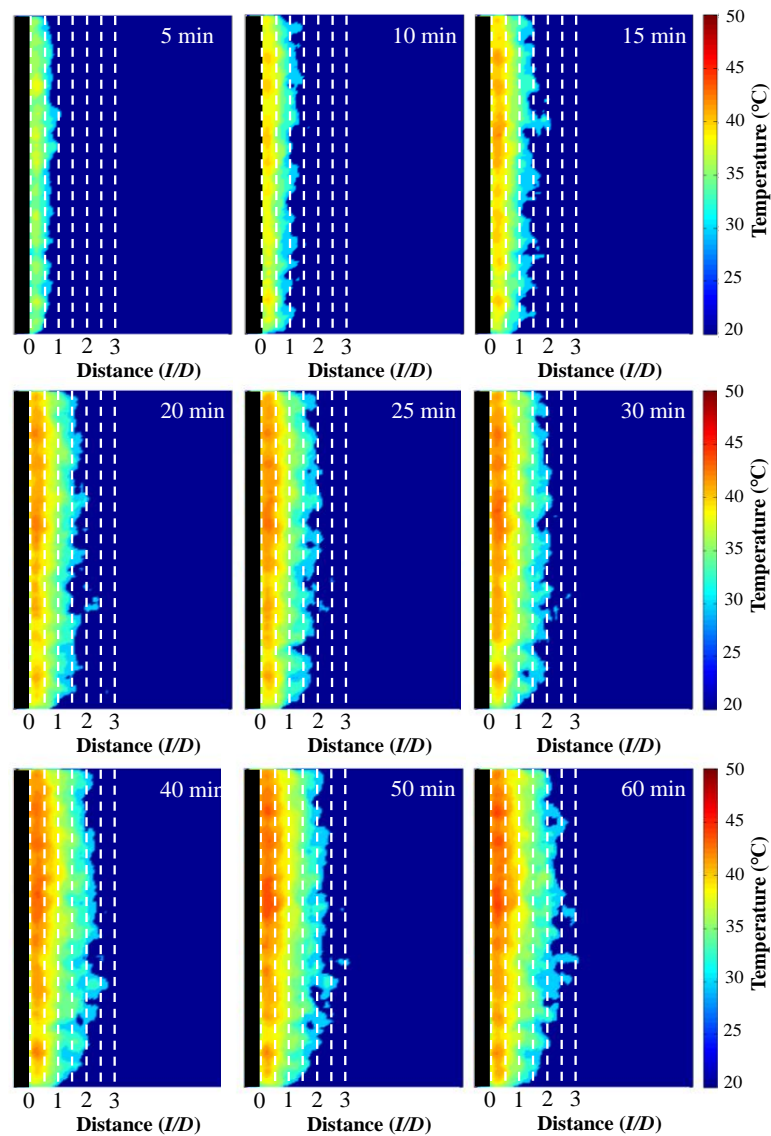


Figure 9. Temperature distribution around pipeline in transparent soil with different times.

When using transparent soil to study the temperature distribution, the test results may have errors due to light conditions, impurities in the transparent soil and other reasons. In order to reduce the test error, the average value of the temperature at the same distance from the pipe wall is taken as the temperature at that distance. The relationships between the temperature and heating time at the distances of $0.5D$, $1.0D$, $1.5D$ and $2D$ are shown in Figure 10. It can be seen that the temperature at different locations increases with heating time, and then tends to be stable. In addition, the temperature of the soil at a distance of $0.5D$ increases rapidly after the start of heating, while the temperature of the soil at distances of $1.0D$, $1.5D$ and $2D$ begins to increase after 5 min, 10 min and 30 min, respectively. It indicates that the influence range of temperature gradually expands with the increase in time. The soil temperatures at different locations all tend to be stable after 60 min.

After the temperature is stable (60 min), the temperature distribution at different distances from the pipe wall is shown in Figure 11. It can be observed that the temperature gradually decreases with the increase in the distance from the pipe wall. The temperature influence range that can be observed is about $2.6D$. At the distance far from $2.6D$, it is difficult to use transparent soil to observe the temperature due to the small temperature change. Moreover, the test results of transparent soil at $0\sim 0.3D$ decreased significantly,

which may be related to the reflection of the model pipe wall. The light reflection of the pipe wall affects the test results.

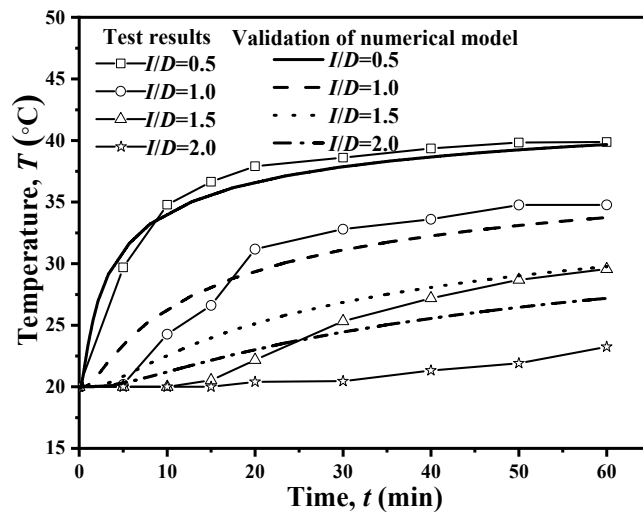


Figure 10. The temperature at different distances (I/D) far from the pipe wall varies with time.

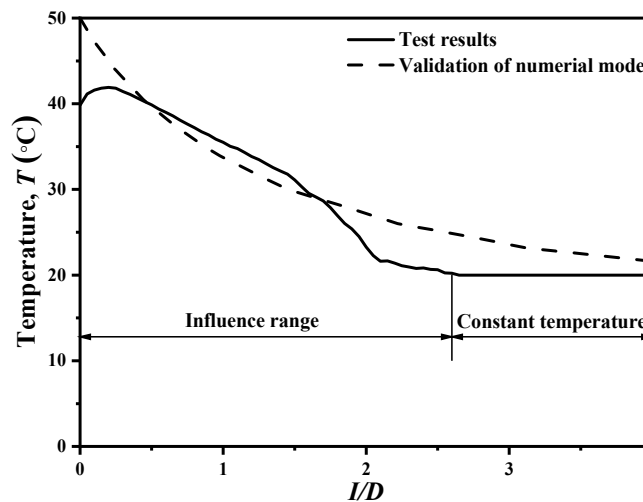


Figure 11. The influence range of pipeline temperature during stable operation in transparent soil.

3.3. Influence of Buried Depth and Pipe Diameter on Temperature Field

To verify the validity of the numerical model, the soil parameters and initial conditions for the transparent soil test were used via the numerical model. Their results are shown in Figures 10 and 11, respectively. It can be seen that numerical simulation results are very close to the results of transparent soil test, indicating that it is feasible to use the numerical model to study the distribution of temperature around the pipeline.

The soil temperature at different locations around the pipeline over time under different buried depths and pipeline diameters are shown in Figures 12 and 13. It can be seen that in the early stage of pipeline operation, the soil temperature increases rapidly. As the soil temperature continues to rise, the heat transferred by the pipeline to the soil is gradually reduced. The rise rate of the soil temperature decreases. The rate and magnitude of temperature rise at point 4 is much lower than that at point 1, which indicates that with the increase in the distance from the pipe wall, the influence of the pipe on the surrounding soil temperature gradually decreases.

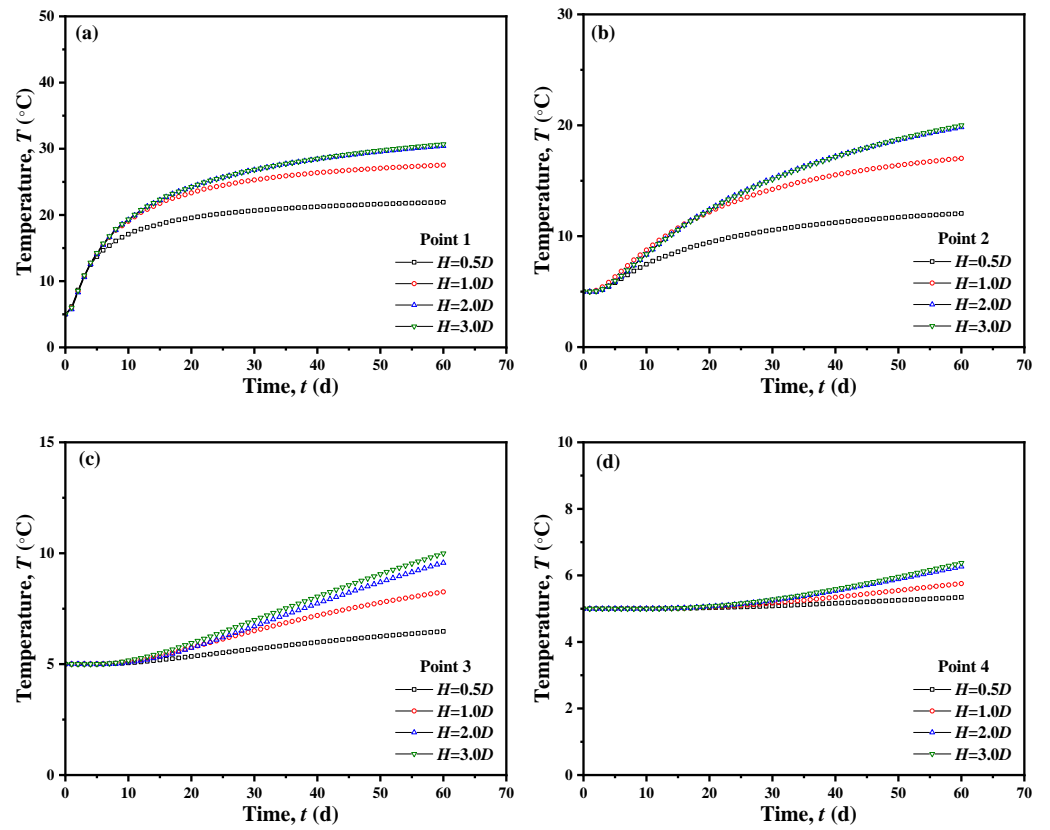


Figure 12. Temperature variation in soil with time at different locations with different buried depths: (a) point 1; (b) point 2; (c) point 3; (d) point 4.

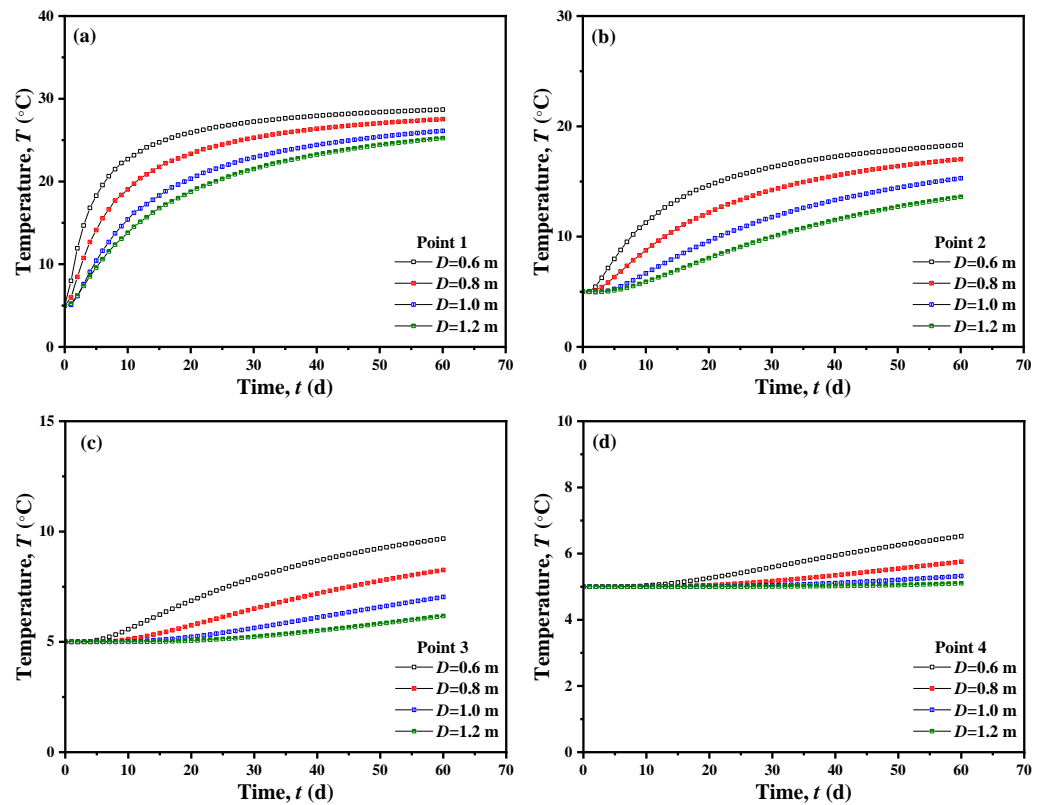


Figure 13. Temperature variation in soil with time at different locations with different diameters: (a) point 1; (b) point 2; (c) point 3; (d) point 4.

Figure 12 also shows that the soil temperature around the pipeline is closely related to the buried depth of the pipeline. As can be seen in Figure 12, the deeper the buried depth of the pipeline, the higher the temperature of the soil around the pipeline. This is influenced by the natural convection between seabed and seawater. The variation in soil temperature at different locations around the pipe with time under different pipe diameters is shown in Figure 13. The diameter of the pipeline affects the rise rate of the soil temperature around the pipeline. The larger the diameter, the slower the rise rate of soil temperature.

After 60 days of heating, the temperature distribution of soil around the pipeline tends to be stable. The temperature distribution around the pipeline during stable operation at different buried depths H is shown in Figure 14. It can be seen from the figure that the soil temperature gradient near the pipe wall is large, indicating that the soil is greatly affected by the pipe temperature. The soil temperature gradient far away from the pipe wall decreases, and the soil is less affected by the pipe temperature. The temperature gradient around the pipeline is relatively small at a small buried depth. With the increase in the buried depth, the temperature gradient tends to be stable, indicating that the influence of natural convection on the temperature field decreases with the increase in the buried depth.

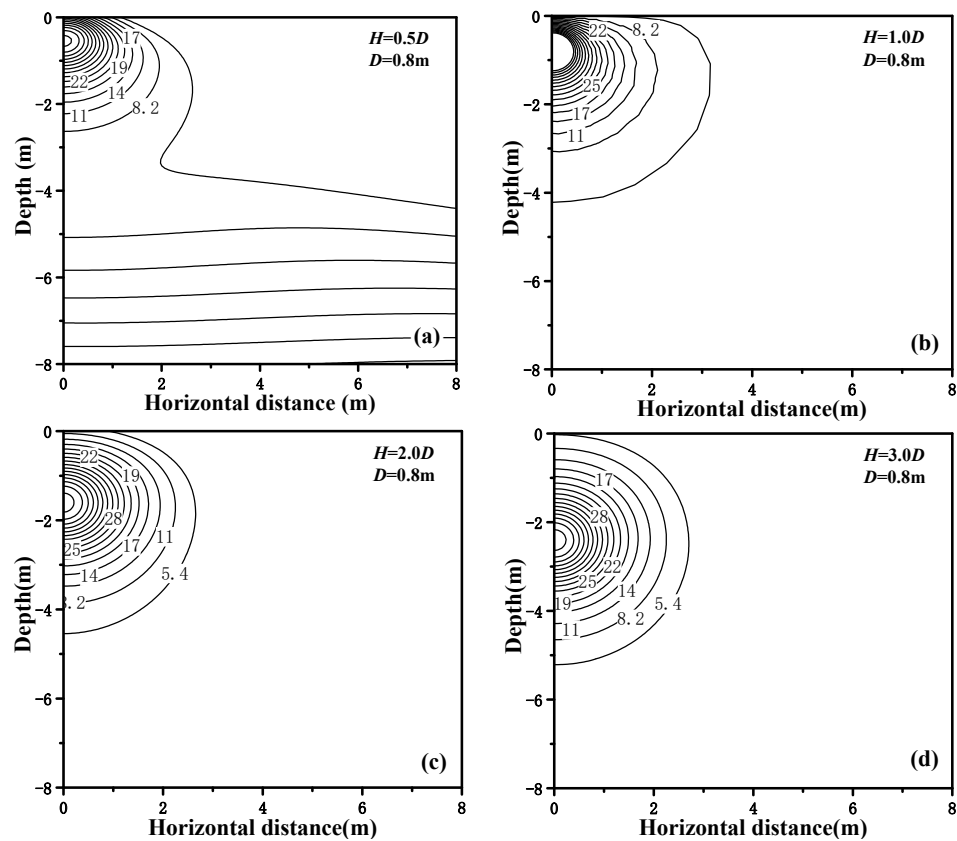


Figure 14. Temperature distribution of soil around pipeline at different buried depths: (a) $H = 0.5D$; (b) $H = 1.0D$; (c) $H = 2.0D$; (d) $H = 3.0D$.

The variation in soil temperature in the horizontal direction of the pipe center during stable operation at different buried depths is shown in Figure 15. It shows that the final influence range of heating on the soil temperature at different buried depths is about $4D$. However, the buried depth has little effect on the influence range of heating. At the same location, the smaller the buried depth, the lower the temperature, and the more obvious the influence of natural convection on the soil temperature.

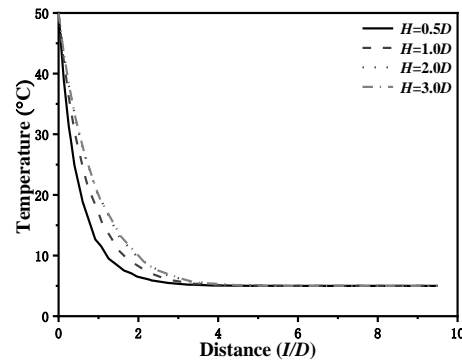


Figure 15. Temperature distribution of soil in horizontal direction of pipeline center at different buried depths.

The temperature distribution of soil around the pipeline with different pipe diameters during stable operation is shown in Figure 16. It can be seen that the contour shape of soil temperature around the pipeline under different pipe diameters is similar. But, the influence distance of heating will increase with the increased in the pipe diameter.

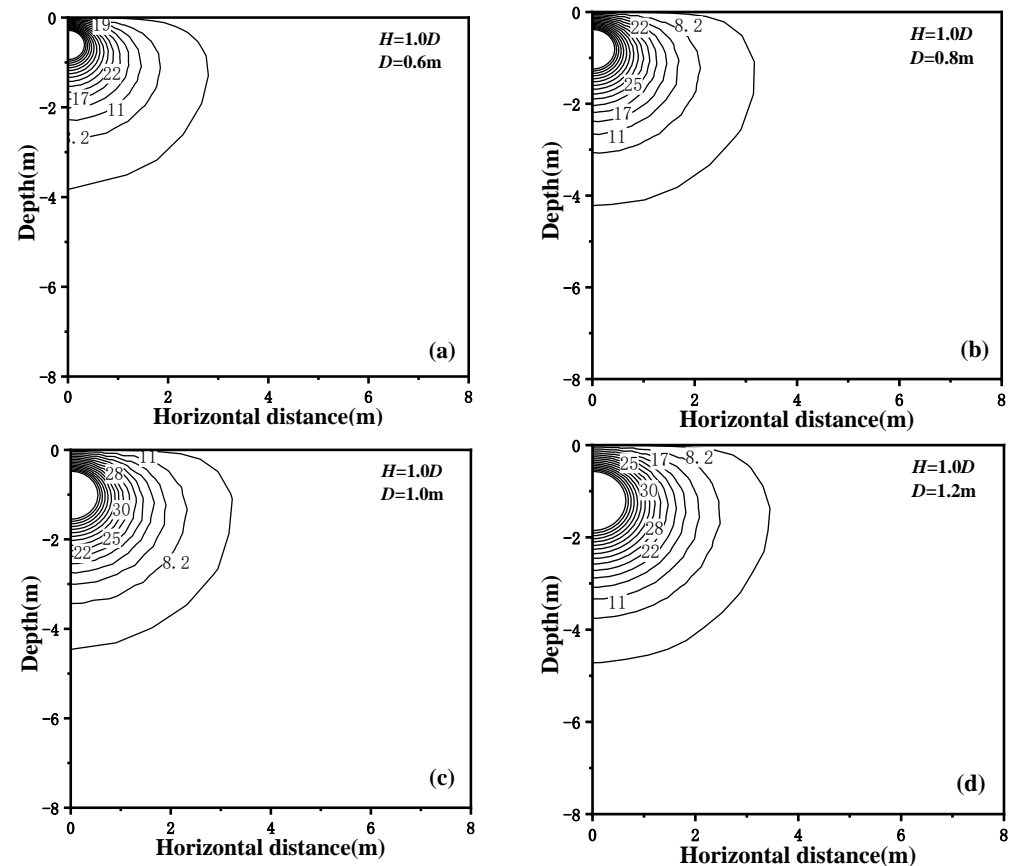


Figure 16. Temperature distribution of soil around pipeline at different diameters: (a) $D = 0.6$ m; (b) $D = 0.8$ m; (c) $D = 1.0$ m; (d) $D = 1.2$ m.

The variation in soil temperature in the horizontal direction of the pipe center during stable operation at different pipe diameters is shown in Figure 17. It shows that the influence range of the heating on the soil temperature under different pipe diameters is also about $4D$. The pipe diameter has little influence on the temperature range of the pipe. At the same distance, the larger the pipe diameter, the lower the soil temperature.

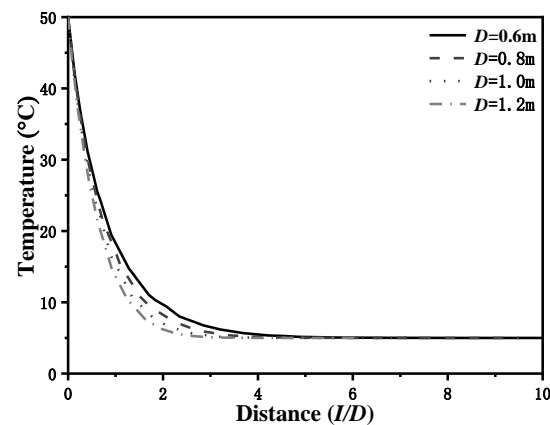


Figure 17. Temperature distribution of soil in horizontal direction of pipeline center at different pipeline diameters.

4. Conclusions

In this paper, an alternative experimental method to realize the visualization research on the temperature of soil around a submarine buried offshore pipeline is proposed based on transparent soil test technology. A set of test apparatuses was built, and the temperature distribution of the soil around the submarine pipeline during the operation was studied. Moreover, the influence of buried depth and pipe diameter on the soil temperature distribution was studied via numerical simulation, considering the natural convection. The following conclusions were obtained:

(1) The relationship between the soil temperature and normalized pixel intensity was established. The normalized pixel intensity varied from 0 to 1 for the temperature of 20 °C to 50 °C. The temperature of transparent soil had a logarithmic relationship with the normalized pixel intensity. It proved the feasibility of using transparent soil test technology to study the soil temperature distribution.

(2) The soil temperature at different locations increased with time, and then tended to be stable. The influence zone of pipeline temperature gradually expanded with the increase in time, and the final observable influence zone extended to a radial distance of $2.6D$. At the distance far from $2.6D$, it was difficult to use transparent soil to observe the temperature due to the small temperature change, which needed further researches to solve these problems.

(3) The shallower the buried depth of the pipeline, the smaller the soil temperature gradient around the pipeline and the more obvious the influence of natural convection of seawater. The contour shape of soil temperature around the pipeline was similar under different buried depths. The influence zone of pipeline temperature was a distance of $4D$ at a temperature difference of 45 °C, which was less effected by the buried depth and pipe diameter.

Author Contributions: Conceptualization, H.L. and Y.S.; methodology, Y.S. and L.G.; software, Y.M., Y.S. and H.L.; validation, L.G. and H.L.; formal analysis, L.G.; investigation, H.L. and Y.M.; resources, H.L., L.G. and Y.S.; data curation, H.L., Y.M., Y.S. and L.G.; writing—original draft preparation, H.L., Y.M. and Y.S.; writing—review and editing, Y.S. and L.G.; visualization, H.L. and Y.M.; supervision, L.G. All authors have read and agreed to the published version of the manuscript.

Funding: This study was funded by Youth Fund of the National Natural Science Foundation of China (52308371), the National Natural Science Foundation of China (51978532) and the Zhejiang Provincial Natural Science Foundation of China (LQ24E080013).

Institutional Review Board Statement: Not applicable.

Informed Consent Statement: Not applicable.

Data Availability Statement: The data presented in this study are available from the corresponding author by request.

Acknowledgments: The findings presented in this article were made possible through the diligent guidance of the authors' supervisor and the invaluable assistance of classmates, as well as the care and help of the teachers in the research group.

Conflicts of Interest: The authors declare no conflicts of interest.

References

1. Yang, X.; Shi, X.; Zhao, J.; Yu, C.; Gao, H.; Chen, A.; Lu, Y.-Z.; Chen, X.; Lin, W.; Zeng, X.; et al. Bottom Water Temperature Measurements in the South China Sea, Eastern Indian Ocean and Western Pacific Ocean. *J. Trop. Oceanogr.* **2018**, *37*, 86–97. [[CrossRef](#)]
2. Yu, J.; An, C.; Tang, Q.; Zhang, J.; Zhang, Y. Heat Transfer Characteristics of Subsea Long-Distance Pipeline Subject to Direct Electrical Heating. *Geoenergy Sci. Eng.* **2024**, *234*, 212679. [[CrossRef](#)]
3. Yuan, Q.; Luo, Y.; Shi, T.; Gao, Y.; Wei, J.; Yu, B.; Chen, Y. Investigation into the Heat Transfer Models for the Hot Crude Oil Transportation in a Long-Buried Pipeline. *Energy Sci. Eng.* **2023**, *11*, 2169–2184. [[CrossRef](#)]
4. Barletta, A.; Zanchini, E.; Lazzari, S.; Terenzi, A. Numerical Study of Heat Transfer from an Offshore Buried Pipeline under Steady-Periodic Thermal Boundary Conditions. *Appl. Therm. Eng.* **2008**, *28*, 1168–1176. [[CrossRef](#)]
5. Lu, T.; Wang, K. Numerical Analysis of the Heat Transfer Associated with Freezing/Solidifying Phase Changes for a Pipeline Filled with Crude Oil in Soil Saturated with Water during Pipeline Shutdown in Winter. *J. Pet. Sci. Eng.* **2008**, *62*, 52–58. [[CrossRef](#)]
6. Rossi di Schio, E.; Lazzari, S.; Abbati, A. Natural Convection Effects in the Heat Transfer from a Buried Pipeline. *Appl. Therm. Eng.* **2016**, *102*, 227–233. [[CrossRef](#)]
7. Li, Y.; Zhou, H.; Liu, H.; Ding, X.; Zhang, W. Geotechnical Properties of 3D-Printed Transparent Granular Soil. *Acta Geotech.* **2021**, *16*, 1789–1800. [[CrossRef](#)]
8. Iskander, M.; Lai, J.; Oswald, C.; Mannheimer, R. Development of a Transparent Material to Model the Geotechnical Properties of Soils. *Geotech. Test. J.* **1994**, *17*, 425–433. [[CrossRef](#)]
9. Zhao, H.; Ge, L. Investigation on the Shear Moduli and Damping Ratios of Silica Gel. *Granul. Matter* **2014**, *16*, 449–456. [[CrossRef](#)]
10. Liu, J.; Iskander, M.G. Modelling Capacity of Transparent Soil. *Can. Geotech. J.* **2010**, *47*, 451–460. [[CrossRef](#)]
11. Sun, Z.; Kong, G.; Zhou, Y.; Shen, Y.; Xiao, H. Thixotropy of a Transparent Clay Manufactured Using Carbopol to Simulate Marine Soil. *J. Mar. Sci. Eng.* **2021**, *9*, 738. [[CrossRef](#)]
12. Downie, H.; Holden, N.; Otten, W.; Spiers, A.J.; Valentine, T.A.; Dupuy, L.X. Transparent Soil for Imaging the Rhizosphere. *PLoS ONE* **2012**, *7*, e44276. [[CrossRef](#)] [[PubMed](#)]
13. Iskander, M.; Bathurst, R.J.; Omidvar, M. Past, Present, and Future of Transparent Soils. *Geotech. Test. J.* **2015**, *38*, 557–573. [[CrossRef](#)]
14. Ads, A.; Bless, S.; Iskander, M. Shape Effects on Penetration of Dynamically Installed Anchors in a Transparent Marine Clay Surrogate. *Acta Geotech.* **2023**, *18*, 3043–3059. [[CrossRef](#)]
15. Ads, A.; Shariful Islam, M.; Iskander, M. Longitudinal Settlements during Tunneling in Soft Clay, Using Transparent Soil Models. *Tunn. Undergr. Space Technol.* **2023**, *136*, 105042. [[CrossRef](#)]
16. Yu, S.; He, F.; Zhang, J. Experimental PIV Radial Splitting Study on Expansive Soil during the Drying Process. *Appl. Sci.* **2023**, *13*, 8050. [[CrossRef](#)]
17. Black, J.A.; Tatari, A. Transparent Soil to Model Thermal Processes: An Energy Pile Example. *Geotech. Test. J.* **2015**, *38*, 752–764. [[CrossRef](#)]
18. Siemens, G.A.; Mumford, K.G.; Kucharczuk, D. Characterization of Transparent Soil for Use in Heat Transport Experiments. *Geotech. Test. J.* **2015**, *38*, 620–630. [[CrossRef](#)]
19. Kong, G.Q.; Li, H.; Hu, Y.X.; Yu, Y.X.; Xu, W.B. New Suitable Pore Fluid to Manufacture Transparent Soil. *Geotech. Test. J.* **2017**, *40*, 658–672. [[CrossRef](#)]
20. Ezzein, F.M.; Bathurst, R.J. A New Approach to Evaluate Soil-Geosynthetic Interaction Using a Novel Pullout Test Apparatus and Transparent Granular Soil. *Geotext. Geomembr.* **2014**, *42*, 246–255. [[CrossRef](#)]
21. Zhang, J.; Stewart, D.P.; Randolph, M.F. Modeling of Shallowly Embedded Offshore Pipelines in Calcareous Sand. *J. Geotech. Geoenviron. Eng.* **2002**, *128*, 363–371. [[CrossRef](#)]
22. Zhang, J.M. Study on the Fundamental Mechanical Characteristics of Calcareous Sand and the Influence of Particle Breakage. Ph.D. Thesis, Chinese Academy of Sciences, Wuhan, China, 2007.
23. Liu, R.; Yan, S.W.; Wang, H.B.; Zhang, J.; Xu, Y. Model tests on soil restraint to pipelines buried in sand. *Chin. J. Geotech. Eng.* **2011**, *33*, 559–565.
24. Kong, G.Q.; Cao, Z.H.; Zhou, H.; Sun, X.J. Analysis of Piles Under Oblique Pullout Load Using Transparent-Soil Models. *Geotech. Test. J.* **2015**, *38*, 725–738. [[CrossRef](#)]

25. Bai, Y.; Niedzwecki, J.M.; Sanchez, M. *Numerical Investigation of Thermal Fields around Subsea Buried Pipelines*; American Society of Mechanical Engineers: New York, NY, USA, 2014.
26. Black, J.A.; Take, W.A. Quantification of Optical Clarity of Transparent Soil Using the Modulation Transfer Function. *Geotech. Test. J.* **2015**, *38*, 588–602. [[CrossRef](#)]

Disclaimer/Publisher’s Note: The statements, opinions and data contained in all publications are solely those of the individual author(s) and contributor(s) and not of MDPI and/or the editor(s). MDPI and/or the editor(s) disclaim responsibility for any injury to people or property resulting from any ideas, methods, instructions or products referred to in the content.